

# ELECTRICAL RESISTIVITY AND ACTIVATION ENERGY OF COBALT ACETATE TETRAHYDRATE DOPED MULLITE

DEBASIS ROY, BISWAJOY BAGCHI, <sup>#</sup>SUKHEN DAS, PAPIYA NANDY

Physics Department, Jadavpur University  
Kolkata- 700 032. India

<sup>#</sup>E-mail: sdasphysics@gmail.com

Submitted November 26, 2011; accepted September 3, 2012

**Keywords:** Nanocomposite, Sol-gel methods, Scanning electron microscopy (SEM), X-ray diffraction (XRD), Electrical resistivity

*Mullite composites have been synthesized at 400°C, 800°C, 1000°C and 1300°C via the sol-gel technique in the presence of cobalt. The electrical resistivity and activation energy of the composites have been measured and their variation with concentration of the metal ion doping has been investigated. The resistivity of doped mullite decreases rapidly from 400°C-800°C more gently from 1000°C-1300°C. The lowering of resistivity is due to the 3d orbital electrons and the concentration of cobalt ions. X-ray analysis confirms the presence of Co<sup>2+</sup> ions in mullite, which entered the octahedral site. The Co<sup>2+</sup> ion which substituted Al<sup>3+</sup> ion in the octahedral site of mullite structure appeared to be efficient in reducing the resistivity. This has been confirmed due to the results of activation energy of resistivity/band gap energy, the E<sub>g</sub> which was lowest for concentration 0.15 M. As the concentration increases, these ions lower the resistivity of mullite to a minimum.*

## INTRODUCTION

Mullite is a highly stable ceramic material with high mechanical strength, low dielectric constant, high creep resistance and low thermal expansion coefficient [1-8]. Typically, mullite formation starts from 1000°C and is completed at about 1600°C, due to solid-state reaction between Al<sub>2</sub>O<sub>3</sub> and SiO<sub>2</sub> particles [9-15]

Synthesis of mullite composites in the presence of various doping agents modifying the mechano-chemical properties has been reported by many authors however, literature concerning the activation energy of resistivity / band gap energy (E<sub>g</sub>) of cobalt doped mullite composites are relatively few [16-22].

This paper deals with the synthesis of mullite composites doped with varying concentrations of cobalt ions and determines the effect of the same on resistivity/activation energy of the composites at temperatures 400°C, 800°C, 1000°C and 1300°C.

The results indicate that the electrical resistivity of composite varies from order 10<sup>10</sup> Ω.cm<sup>-1</sup> at 400°C to order 10<sup>5</sup> Ω.cm<sup>-1</sup> at 1300°C. As the temperature is increasing, the resistivity is decreasing [23, 24].

The lattice parameters (*a*, *b*, *c*) and unit cell volume change due to the incorporation of dopants. Synthesis of mullite composites in the presence of various doping agents has shown that these structural parameter changes do not depend on the nature of the dopants [25, 26].

The unit cell parameter according to Chaudhuri et al. [23], *b* axis and *c* axis increases steadily, but contraction took place along the *a* axis. For undoped mullite (*a* = 7.544 Å, *b* = 7.687 Å and *c* = 2.881 Å and unit cell volume 167.07 Å<sup>3</sup>) and for doped mullite it has been observed that the *a*-axis as well as the *b*-axis of mullite show elongation, but the *c*-axis almost remains constant for sintered gels at 1000°C and 1300°C [23,24].

## EXPERIMENTAL

Mullite precursor gels are prepared from aluminium nitrate nonahydrate (Al(NO<sub>3</sub>)<sub>3</sub>·9H<sub>2</sub>O) extra pure (Merck, India), aluminium isopropoxide (Al(-O-i-Pr)<sub>3</sub>) puriss (Spectrochem Pvt. Ltd., India.), tetra ethyl orthosilicate (Si(OC<sub>2</sub>H<sub>5</sub>)<sub>4</sub>), (Merck, Germany) and cobalt acetate tetrahydrate (CH<sub>3</sub>COO)<sub>2</sub> Co.4H<sub>2</sub>O (Qualigens Fine Chemicals, India).

For the preparation of precursor gels for mullite synthesis, Al (-O-i-Pr)<sub>3</sub> and Si(OC<sub>2</sub>H<sub>5</sub>)<sub>4</sub> were added simultaneously to 0.5 M solution of Al (NO<sub>3</sub>)<sub>3</sub>·9H<sub>2</sub>O dissolved in 20 ml of distilled water. The molar ratio of Al (-O-i-Pr)<sub>3</sub>/Al (NO<sub>3</sub>)<sub>3</sub>·9H<sub>2</sub>O was 7 : 2 and mole ratio of Al/Si was 3:1 [14].

Doped gels were prepared by adding corresponding metal salt to the original solution in the ratio Al: Si: M, where M is the concentration of the cobalt

salt in molarity. In the final solution, M was varied as  $M = 0.002 (G_1)$ ,  $0.02 (G_2)$ ,  $0.10 (G_3)$ ,  $0.15 (G_4)$  and  $0.2 M (G_5)$  [12, 13].

Gel formation was completed after stirring the solution for 3 hours and ageing the sol overnight at  $60^\circ\text{C}$ . The gel was then dried at  $110^\circ\text{C}$  and after grinding, it takes the form of freely flowing powder. The samples were then pelletized in disc form of 30 mm diameter and 3 mm thickness and sintered at  $400^\circ\text{C}$ ,  $800^\circ\text{C}$ ,  $1000^\circ\text{C}$  and  $1300^\circ\text{C}$  for 3 hr in a muffle furnace under air atmosphere at the heating rate of  $10^\circ\text{C}/\text{minute}$  [15-18].

The fired pellets were then coated by silver paste on both sides for electrical measurements.

The silver-coated discs were placed in a press-contact type teflon holder to minimize leakage resistance from the holder. The chamber was made vacuum-tight and properly shielded [23].

#### Instrumentation

X-ray Powder Diffractometer of D8, Bruker AXS, Wisconsin, USA, using  $\text{Cu K}\alpha$  radiation ( $1.5418 \text{ \AA}$ ) and operating at 40 kV with a scan speed of 1 s/step, analyzed phase identification of the samples sintered at  $400^\circ\text{C}$ ,  $800^\circ\text{C}$ ,  $1000^\circ\text{C}$  and  $1300^\circ\text{C}$ .

The characteristic stretching and bending modes of vibration of chemical bonds of a sample can be effec-

tively evaluated by spectroscopic methods. 1 % of the sample was mixed with spectroscopy grade KBr, pelletized and analyzed by FTIR spectroscopy (FTIR-8400S, Shimadzu).

Electrical resistivity measurements of the sintered gels were carried out by electrometer. A constant DC voltage (V) of about 1.5 V was applied from a battery across the sample. The voltage (V) across the input resistance was measured by the electrometer.

Morphology of the sintered gels were observed by Field Emission Scanning Electron Microscope (FESEM, model JSM 6700F, JEOL Ltd. Tokyo, Japan).

#### RESULTS AND DISCUSSION

X-ray diffractograms of doped sintered gels shows considerable enhancement in mullite phase at  $400^\circ\text{C}$ ,  $800^\circ\text{C}$ ,  $1000^\circ\text{C}$  and  $1300^\circ\text{C}$  respectively. The metal cation  $\text{Co}^{2+}$  had a positive effect on the growth of mullite (JCPDS#15-776) [27] and increases with the increase of concentration of the metal ion at  $400^\circ\text{C}$ ,  $800^\circ\text{C}$ ,  $1000^\circ\text{C}$  and  $1300^\circ\text{C}$  (Figure 1). The ‘mineralizing’ effect of transition metals on phase transformation of mullite is well documented by other authors [16-18]. Interaction of the metal ion with the alumina and silica component of the gel is implicated in accelerated transformation to mullite phase [16, 21, 26].

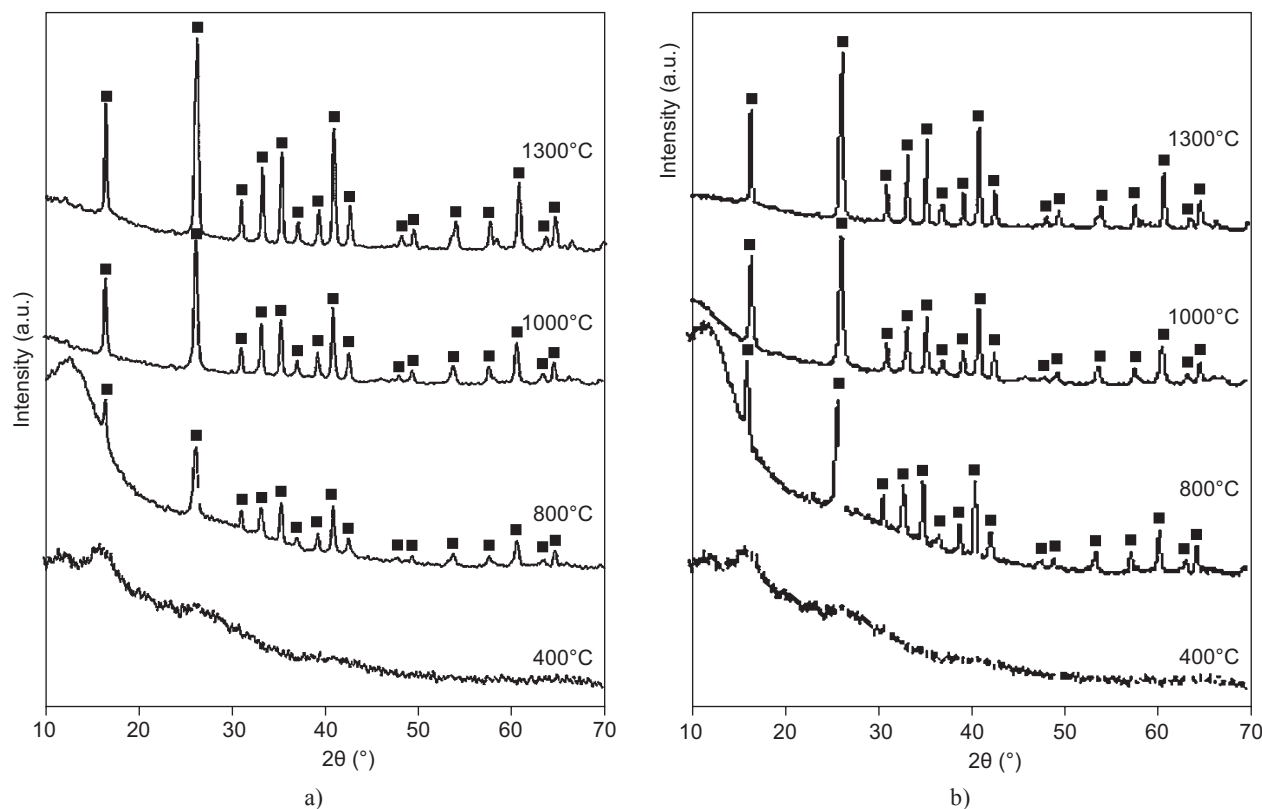
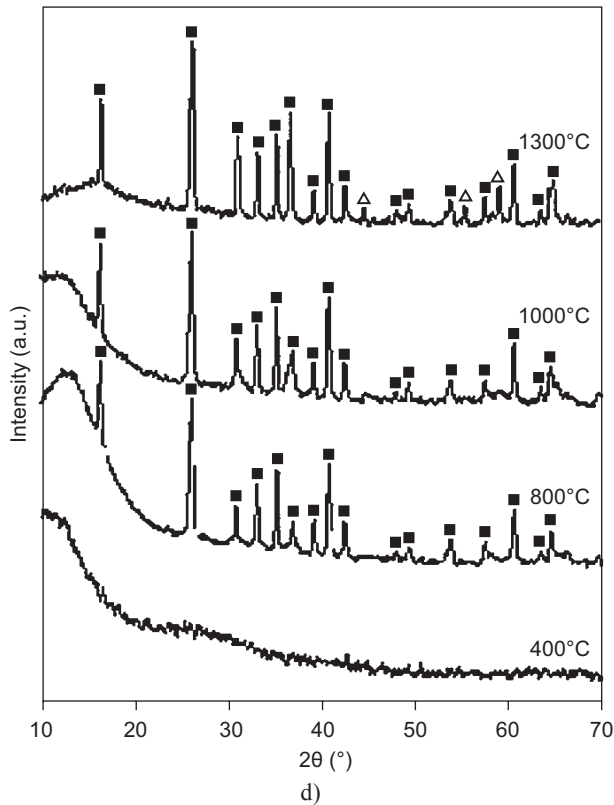
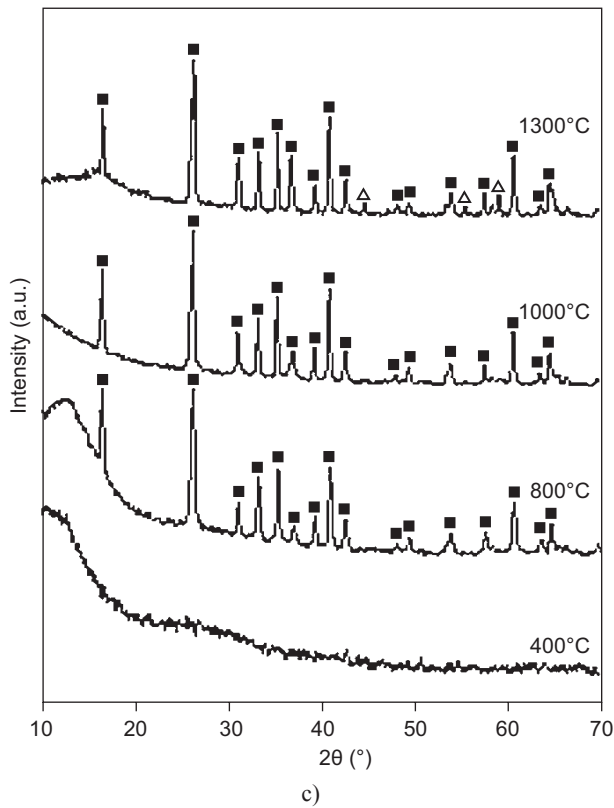


Figure 1. X-ray diffraction pattern of mullite precursor gels sintered at  $400^\circ\text{C}$ ,  $800^\circ\text{C}$ ,  $1000^\circ\text{C}$  and  $1300^\circ\text{C}$  containing increasing concentration of cobalt (continue on next page).

From the diffractograms, it was found that with the increase of metal concentration of doped metal, phase transformation in the composite increases. In the



diffractograms of G<sub>3</sub>, G<sub>4</sub> and G<sub>5</sub> samples, apart from mullite, α-Al<sub>2</sub>O<sub>3</sub> (JCPDS#46-1212) [28] reflections were observed and in G<sub>5</sub> CoAl<sub>2</sub>O<sub>4</sub> (JCPDS# 44-0160) [29] phases are observed (Figure 1e).

Characteristic bands at wave numbers are observed around 560, 730, 840, 1060 and 1130 cm<sup>-1</sup>, see Figure 2 [16]. All the characteristic bands of mullite - 561 (AlO<sub>6</sub>), 741 (AlO<sub>4</sub>), 837 (AlO<sub>4</sub>), 900 (AlO<sub>4</sub> - stretching mode) and 1130 cm<sup>-1</sup> (Si-O stretching mode) appear in samples G<sub>1</sub>, G<sub>2</sub>, G<sub>3</sub>, G<sub>4</sub> and G<sub>5</sub>. Vibration modes corresponding to doped cobalt oxide bonds were observed in the FTIR spectra.

According to, Ohm's law the current (*I*) in the circuit is:

$$I = V/R \quad (1)$$

where *V* is voltage, *I* is current, and *R* is the resistance of the load, in this case the sample of cobalt doped mullite. Therefore, the resistance (*R*) of the sample was calculated as:

$$R = V/I \quad (2)$$

In the time of measurement of resistance of each sample, the voltage of the battery was checked. The ρ resistivity of a material can be calculated using the relationship:

$$\rho = R (A/l) \quad (3)$$

where ρ is the material bulk resistivity, *l* is the sample length, and *A* is the sample's cross-sectional area perpendicular to the current flow.

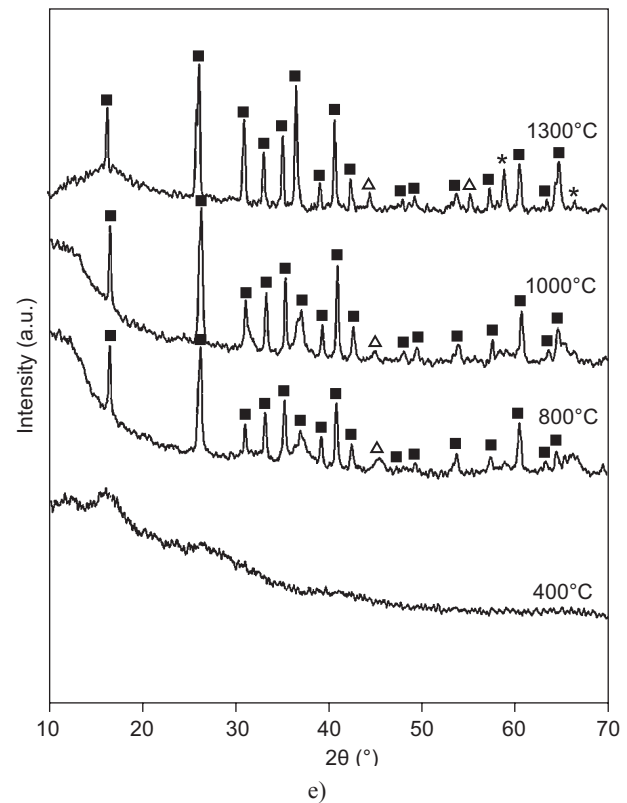
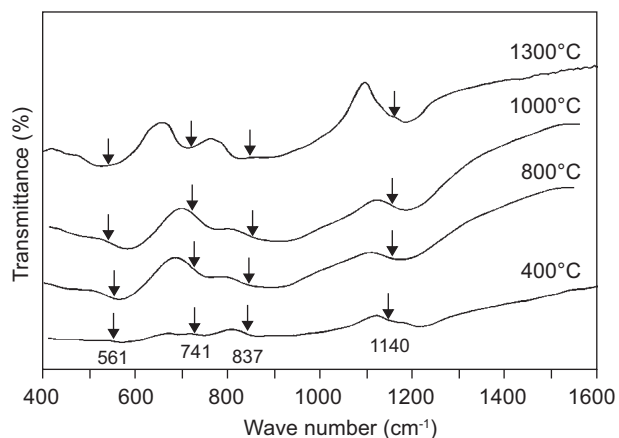


Figure 1. X-ray diffraction pattern of mullite precursor gels sintered at 400°C, 800°C, 1000°C and 1300°C containing increasing concentration of cobalt.

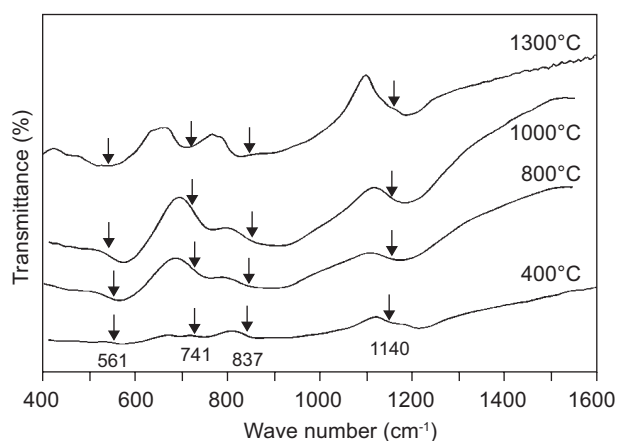
The electrical conductivity of the samples were described by the Arrhenius equation as follows:

$$\sigma = \alpha e^{E_g/kT} \quad (4)$$

where  $\sigma$  is the electrical conductivity given by  $\sigma = 1/\rho$ ,  $\alpha$  is a pre-exponential factor,  $T$  is the absolute temperature,  $k$  is the Boltzmann constant, and  $E_g$  is the material's activation energy.



a)



b)

The electrical resistivity of the samples were described as

$$\rho = 1/\sigma \quad (5)$$

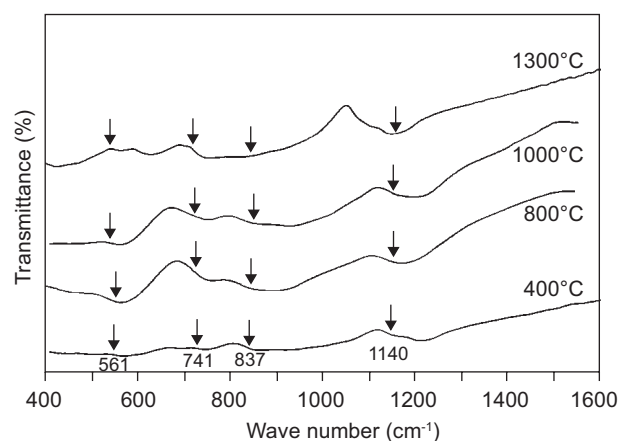
where  $\rho$  is the material bulk resistivity and  $\sigma$  is the electrical conductivity [23-25].

A plot of  $\log_{10} \rho$  versus  $1/T \cdot 10^4$  was drawn for each sample at temperatures 400°C, 800°C, 1000°C and 1300°C, see Figure 3. The plots show a linear increase with the reciprocal temperature.

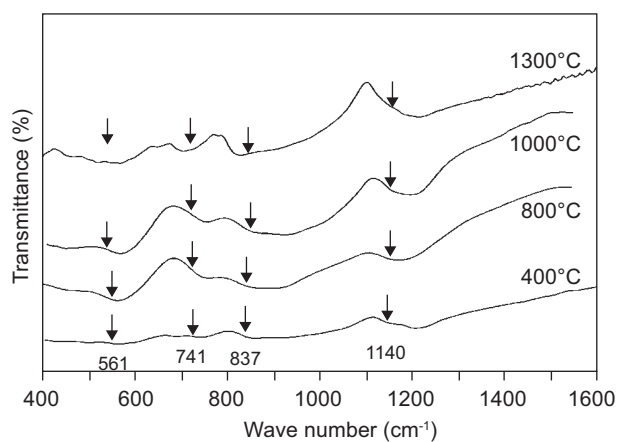
From the  $\log_{10} \rho$  vs sintering temperature (°C) curve, resistivity decreases with increasing temperature. It has been observed that for concentration  $G_1$  and  $G_2$  the resistivity decreases sharply in the lower temperature range, but in the higher temperature range  $G_3, G_4, G_5$  decrease rapidly.  $G_3$  exhibits the lowest resistivity  $5.46 \cdot 10^5 \Omega \text{ cm}$  (Figure 4). The  $\text{Co}^{2+}$  ions entered the mullite lattice in different positions and substituted  $\text{Al}^{3+}$  ion.

The activation energy of the samples were calculated in eV unit from the slope of the plot as follows:

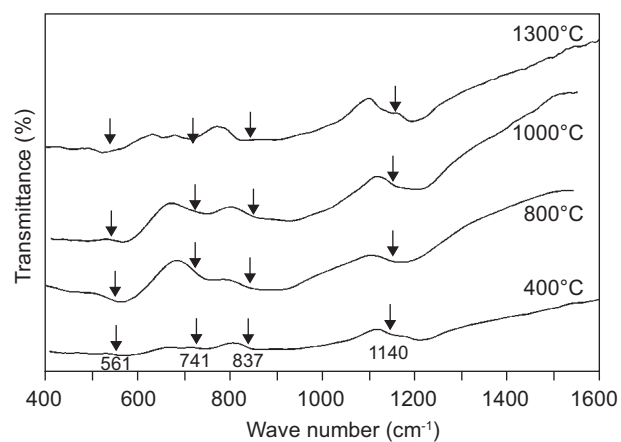
$$E_g = \text{slope} \times 4.606 \times 8.62 \times 10^{-5} \text{ eV} \quad (6)$$



d)



c)



e)

Figure 2. FTIR bands of mullite precursor gels sintered at 400°C, 800°C, 1000°C and 1300°C containing increasing concentration of cobalt.

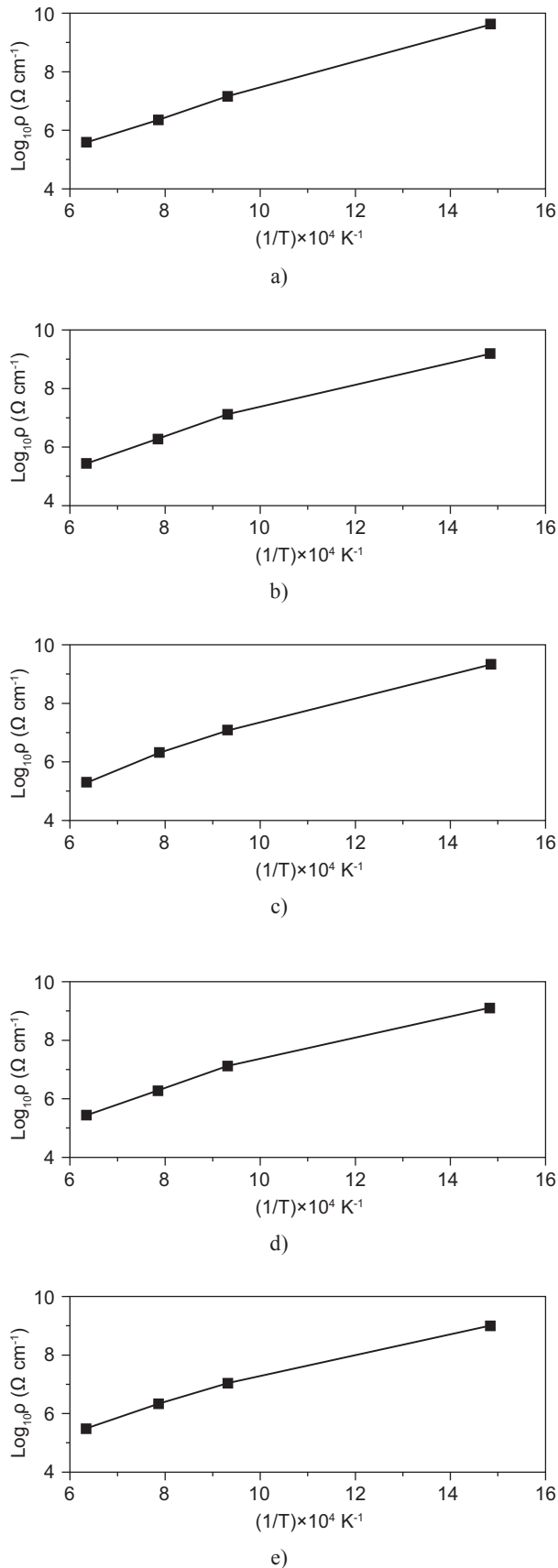


Figure 3. Resistivity ( $\log_{10} \rho$ ) versus  $1/T \times 10^{-4}$  graph of mullite precursor gels sintered at 400°C, 800°C, 1000°C and 1300°C containing increasing concentration of cobalt.

From the  $E_g$  vs concentration curve,  $E_g$  decreases with concentration and becomes minimum at 0.15M.

The substitution of  $\text{Al}^{3+}$  ion in the mullite lattice by  $\text{Co}^{2+}$  ion disturbed the electro neutrality of the composite. As a result probably there will be formation of a hole when  $\text{Al}^{3+}$  ion is replaced by  $\text{Co}^{2+}$  ion in the mullite structure [23, 24, 25]. It was observed that  $\text{Co}^{2+}$  ion could not substitute  $\text{Al}^{3+}$  ion in mullite but remained there as a cluster. The lowering of resistivity is due to the 3d orbital electrons and the concentration of cobalt ions. The  $\text{Co}^{2+}$  ion which substituted  $\text{Al}^{3+}$  ion in the octahedral site of mullite structure appeared to be efficient in reducing the resistivity. [23,35] There are two possibilities of increase of  $E_g$  after attaining its minimum value at 0.15M, either complete incorporation of cobalt in the mullite structure or dissolution of cobalt ions in the Si-rich glassy phase. The dissolution of cobalt ions in the glassy phase should dominate over the incorporation of cobalt ions into mullite.

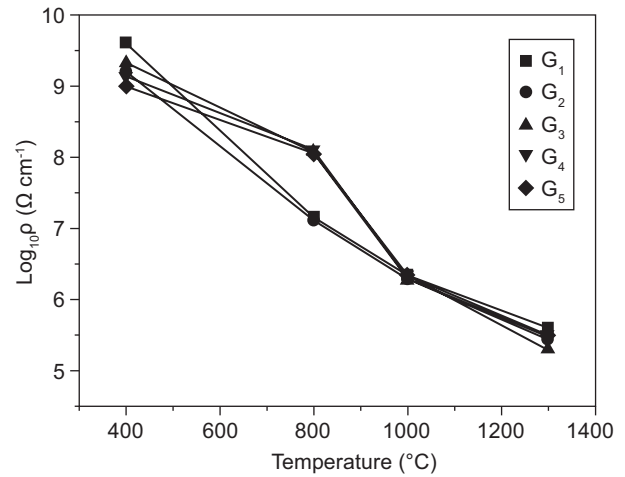


Figure 4. Resistivity versus Temperature ( $^{\circ}\text{C}$ ) of mullite precursor gels sintered at 400°C, 800°C, 1000°C and 1300°C containing increasing concentration of cobalt.

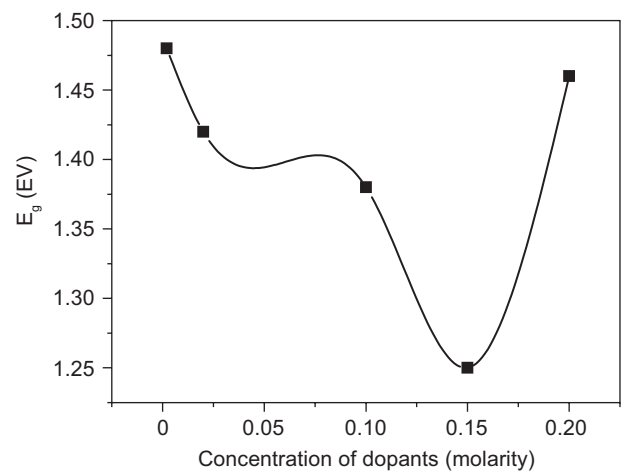


Figure 5. Activation energy ( $E_g$ ) vs concentration curve of mullite precursor gels sintered at 400°C, 800°C, 1000°C and 1300°C containing increasing concentration of cobalt.

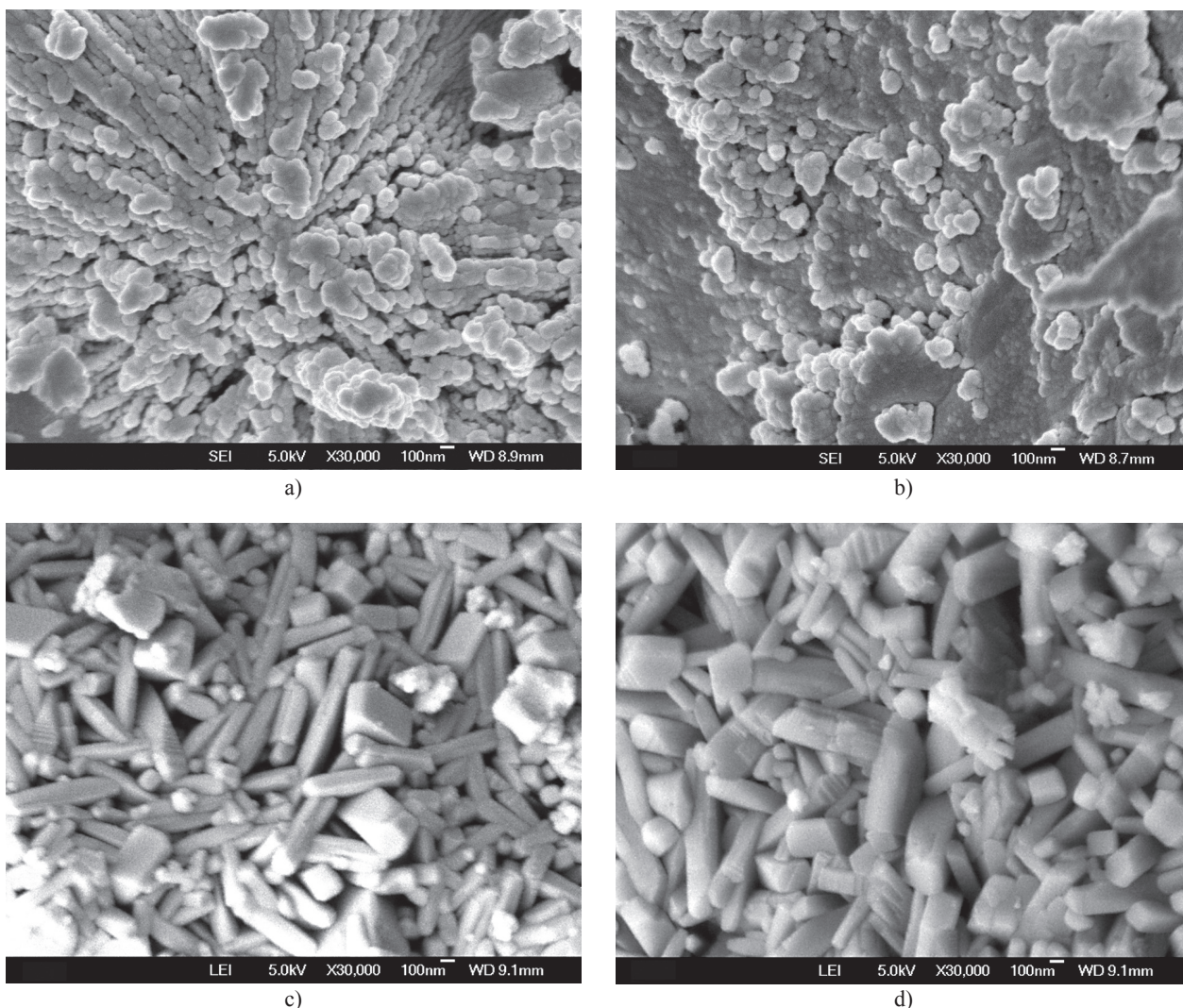


Figure 6. FESEM of mullite precursor gels doped with Cobalt sample  $G_1$  and sample  $G_5$  sintered at  $1000^\circ\text{C}$  and  $1300^\circ\text{C}$ .

Mullite samples, therefore, behave like nonmetallic electrical conductors, because their conductivity rises faster at lower temperature but slows down at higher temperature.

The morphology of mullite particles with lowest ( $G_1$ ) and highest ( $G_5$ ) concentrations of  $\text{Co}^{2+}$  sintered at  $1000^\circ\text{C}$  and  $1300^\circ\text{C}$  was investigated by FESEM.

The micrograph for  $G_1$  shows almost round particles of mullite of an average size of 200 nm. Numerous smaller particles can also be seen along with amorphous aggregates and see Figure 6a,b [12, 30, 31].

$G_5$  samples shows distinct acicular morphology of mullite crystals of size 600 nm embedded in the matrix, see Figure 6c,d. The mullite content and crystallization in all the  $G_5$  samples were greater than in  $G_1$  composites, indicating the catalytic effect of the  $\text{Co}^{2+}$  ions [16, 21].

## CONCLUSION

Cobalt doped mullite composites have been synthesized by the sol-gel technique, their phase evolution,

band gap activation energy and unit cell parameter has been investigated. The results showed that with increase in  $\text{Co}^{2+}$  concentration the crystallization of mullite was enhanced, which is evident from X-ray diffraction and FESEM of the composites. In terms of unit cell parameter, the  $a$ -axis and  $b$ -axis show elongation, but the  $c$ -axis almost remains constant. The activation energy of resistivity/band gap energy,  $E_g$ , attains a minimum value 1.25 eV at 0.15 M concentration. It has been observed that from  $1000^\circ\text{C}$ , the resistivity as well as the band gap energy corresponds to semiconductors.

## Acknowledgement

*We are grateful to the members of the, Department of Science and Technology and University Grant Commission (PURSE program), Government of India, for their assistance.*

## References

1. Aksay I.A., Dabbs D.M., Sarikaya M.: *J. Am. Ceram. Soc.* **74**, 2343 (1991).
2. Rahman S., Freimann S. in: *Mullite*, p. 46, Ed. Schneider H, Komarneni S., Wiley-VCH, Weinheim 2005.
3. Schreuer J., Hildmann B., Schneider H.: *J. Am. Ceram. Soc.* **89**, 1624 (2006).
4. Schneider H., Schreuer J., Hildmann B.: *J. Eur. Ceram. Soc.* **28**, 329 (2008).
5. Perera D.S., Allott G.: *J. Mater Sci Lett.* **4**, 1270 (1985).
6. Davis R.F., Pask J.A., Somiya S.: *J. Am. Ceram. Soc.* Westerville (1990).
7. Schmucker M., Schneider H. In *Mullite*, p. 93, Ed. Schneider H., Komarneni S., Wiley-VCH, Weinheim 2005.
8. Vol'khin V.V., Kazakova I.L., Pongratz P., Halwax E.: *Inorg Mater.* **36**, 375 (2000).
9. Chen Y.F., Wang M.C., Hon M.H.: *J. Eur. Ceram. Soc.* **24**, 2389 (2004).
10. Sahnoune F., Chegaar M., Saheb N., Goeriot P., Valdivieso F.: *Appl. Clay Sci* **38**, 304 (2008).
11. Pascual J., Zapatero J.: *J. Am. Ceram. Soc.* **83**, 2677 (2000).
12. Tang Y.F., Ling Z.D., Lu Y.N., Li AD., Ling HQ., Wang YJ., Shao Y.: *Mater. Chem. Phys.* **75**, 265 (2002).
13. Viswabaskarana V., Gnanama F.D, Balasubramanian M.: *Ceram. Inter.* **28**, 557 (2002).
14. Viswabaskarana V., Gnanama F.D, Balasubramanian M.: *Ceram. Inter.* **29**, 561 (2003).
15. Viswabaskarana V., Gnanama F.D, Balasubramanian M.: *Appl. Clay Sci.* **25**, 29 (2004).
16. Bagchi B., Das S., Bhattacharya A., Basu R., Nandy P.: *J. Sol-Gel. Sci. Technol.* **55**, 135 (2010).
17. T.Martišius., R.Giraitis.: *J. Mater. Chem.* **13**, 121 (2002).
18. S.Aza R., Moya S.J., Epicier T., Fantozzi G.: *J. Mat. Sci. Lett.* **9**, 1400 (1990).
19. Torecillas Imose M., Takano Y., Yoshinaka M., Hirota Yamaguchi K.O.: *J. Am. Ceram. Soc.* **81**, 1537 (1998).
20. Kong L.B., Zhang T.S., Ma J., Boey F.: *J. Alloys. Compd.* **359**, 292 (2003).
21. Bagchi B., Das S., Bhattacharya A., Basu R., Nandy P.: *J. Am. Ceram. Soc.* **92**, 748 (2009).
22. Esharghawi A., Penot C., Nardou F.: *J. Eur. Ceram. Soc.* **29**, 31 (2009).
23. Chaudhuri S. P., Patra S. K., Chakraborty A. K.: *J. Eur. Ceram. Soc.* **19**, 2941 (1999).
24. Kurajica Stanislav., Tkalcec Emilija., Schmauch Joerg.: *J. Eur. Ceram. Soc.* **27**, 951 (2007).
25. Murthy M. K., Hummel F. A.: *J. Am. Ceram. Soc.* **43**, 267 (1960).
26. Cameron W. E.: *Am. Ceram. Soc. Bull.* **56**, 1003 (1977).
27. Kong L.B., Zhang T.S., Ma J., Boey F.: *J. Eur. Ceram. Soc.* **23**, 2247 (2003).
28. Ferreira da Silva M.G.: *J. Sol-Gel. Sci. Technol.* **13**, 987 (1998).
29. Tkalcec E., Kurajica S., Schmauch J.: *Journal of Non-Crystalline Solids*, **353**, 2837 (2007).
30. Weizhong L., Qiu Qi., Wang Fang., Wei S., Liu Bo., Luo Z.: *Ultrasonic Sonochemistry* **17**, 793 (2010).
31. Baranwal R., Villar M. P., Garcia R., Laine R.M.: *J. Am. Ceram. Soc.* **84**, 951 (2001).